ARTICLE

Age differences in brain structural and metabolic responses to binge ethanol exposure in fisher 344 rats

Natalie M. Zahr[1,2], Edith V. Sullivan[1,2], Kilian M. Pohl[1,2] and Adolf Pfefferbaum[1,2]

An overarching goal of our research has been to develop a valid animal model of alcoholism with similar imaging phenotypes as those observed in humans with the ultimate objective of assessing the effectiveness of pharmacological agents. In contrast to our findings in humans with alcohol use disorders (AUD), our animal model experiments have not demonstrated enduring brain pathology despite chronic, high ethanol (EtOH) exposure protocols. Relative to healthy controls, older individuals with AUD demonstrate accelerating brain tissue loss with advanced age. Thus, this longitudinally controlled study was conducted in 4-month old (equivalent to ~16-year-old humans) and 17-month old (equivalent to ~45-year-old humans) male and female Fisher 344 rats to test the hypothesis that following equivalent alcohol exposure protocols, older relative to younger animals would exhibit more brain changes as evaluated using in vivo structural magnetic resonance imaging (MRI) and MR spectroscopy (MRS). At baseline, total brain volume as well as the volumes of each of the three constituent tissue types (i.e., cerebral spinal fluid (CSF), gray matter, white matter) were greater in old relative to young rats. Baseline metabolite levels (except for glutathione) were higher in older than younger animals. Effects of binge EtOH exposure on brain volumes and neurometabolites replicated our previous findings in Wistar rats and included ventricular enlargement and reduced MRS-derived creatine levels. Brain changes in response to binge EtOH treatment were more pronounced in young relative to older animals, negating our hypothesis. Higher baseline glutathione levels in female than male rats suggest that female rats are perhaps protected against the more pronounced changes in CSF and gray matter volumes observed in male rats due to superior metabolic homeostasis mechanisms. Additional metabolite changes including low inositol levels in response to high blood alcohol levels support a mechanism of reversible osmolarity disturbances due to temporarily altered brain energy metabolism.

INTRODUCTION

In humans, long-term, excessive alcohol consumption results in a variety of somatic and central nervous system (CNS) insults [e.g., 1, 2]. In vivo brain structural magnetic resonance imaging (MRI) of uncomplicated alcoholism (that is, alcohol use disorder (AUD) absent clinically diagnosable consequences of chronic alcohol consumption such as Wernicke's encephalopathy) commonly reveals tissue shrinkage in frontally distributed cortical regions [3–5] and subcortical regions including striatum [6–8] and thalamus [9, 10]. Factors that contribute to persistent or accelerated brain volume abnormalities are still being identified but likely include alcohol consumption variables of frequency and amount drunk, age at onset of alcohol misuse, and conditions resulting from years of abusive drinking, such as withdrawal signs and symptoms [11] and alcoholism-related nutritional deficiencies [12, 13]. Perhaps the most salient factor is age, which may render the older brain especially vulnerable to insult from other factors, including excessive alcohol consumption and attendant events [14]. Interaction of normal aging and alcoholism has been borne out in several cross-sectional [15–17] and longitudinal [18–20] studies in which accelerated volume declines appear by approximately age 45 years in alcohol-dependent groups. Assessing the association between age-alcoholism interactions

and brain structure has new urgency considering current epidemiologic data indicating a major increase, measured throughout a decade, in the prevalence of AUD in individuals aged 65 years or older [21, 22].

Animal models of alcoholism offer the opportunity to investigate biological mechanisms of dependence, tolerance, and neuroadaptation, with the potential to test pharmacological and behavioral rehabilitation therapies. Given a number of previous studies that demonstrated similar, but non-enduring patterns of neuroimaging changes in response to high blood alcohol levels (BALs) [e.g., 23–28] we hypothesized that older animals may be necessary to observe persistent pathology [cf., 29]. Thus, the current set of experiments builds upon several previous studies that have used the modified Majchrowicz ethanol (EtOH)-intoxication model to achieve high BALs and longitudinally examine gross brain structure and metabolite responses in rats [24–26, 30]. Because human studies have demonstrated normalization of alcoholism-induced changes in metabolite levels with even short-term abstinence [e.g., 31, 32], cross-sectional, in vivo neurochemical differences examined at a single time point between AUD and healthy control individuals can be challenging to capture [33], but may provide insight into underlying mechanisms of pathology [e.g., 34] and contribute to CNS drug

[1]Neuroscience Program, SRI International, Menlo Park, CA 94025, USA and [2]Department of Psychiatry & Behavioral Sciences, Stanford University, School of Medicine, Stanford, CA 94305, USA
Correspondence: Natalie M. Zahr (nzahr@stanford.edu)

Age differences in brain structural and metabolic responses to binge…
NM Zahr et al.

369

development [e.g., 35]. Multi-modal imaging of animal models, particularly MR Imaging (MRI) and Spectroscopy (MRS) studies— with the ability to measure changes pre- and post- exposure longitudinally—permit speculation regarding mechanism [e.g., 36, 37]. Structural and metabolic changes in response to high BALs achieved by binge (intragastric gavage) EtOH exposure have been consistent across our studies conducted in wild-type Wistar rats [24–26] and include ventricular enlargement [greater cerebrospinal fluid (CSF) volume], lower levels of N-acetyl aspartate [NAA, a marker of neuronal integrity, 38] and total creatine [tCr, energy buffer/shuttle, 38], and higher levels of choline containing compounds [Cho, involved in phospholipid synthesis and degradation, 38] together interpreted as reflecting altered brain energy utilization, disturbed osmolarity, or loss of white matter integrity [26]. While reliable, such changes are transient: following 1 week of recovery, ventricular volume and levels of NAA, tCr, and Cho return to baseline levels, no longer distinguishing control and EtOH-exposed animals. Thus, the first aim of the current study was to determine whether advanced age in rats, equivalent to ~45 human years, would produce more enduring brain structural and biochemical changes to alcohol exposure.

An additional source of variability contributing to brain abnormalities in AUD is sex. Although some literature has suggested that women are more vulnerable than men to the pathological effects of alcohol [39–42], other studies found that alcoholic women do not show disproportionately greater deficits than alcoholic men [43–45]. The rodent literature suggests that female relative to male rats of several strains drink more alcohol [46, 47, but see: 48–50]; but that male relative to female rats show greater evidence for withdrawal [51–54]. Thus, a second aim of the current study was to evaluate sex effects on brain structural and biochemical changes in response to alcohol exposure.

To accomplish these goals, 4-month old equivalent to ~16-year-old humans and 17-month old equivalent to ~45-year-old humans [55], male and female Fisher 344 rats were evaluated in a longitudinally controlled study using in vivo structural MRI and metabolic MRS. Specifically, these experiments tested the hypothesis that following equivalent alcohol exposure protocols, older relative to younger animals and male relative to female animals would exhibit more brain changes.

MATERIALS AND METHODS
Ethics statement
All experimental procedures were conducted in accordance with the Guide for the Care and Use of Laboratory Animals of the National Institutes of Health. The Institutional Animal Care and Use Committees at SRI International and Stanford University approved all procedures.

Animals and treatment
Fisher 344 rats were acquired from the National Institute of Aging (https://ros.nia.nih.gov/). Experiments were conducted in two consecutive waves of 28 animals each comprising 14 young (~4 months, 7 female) and 14 old (~17 months, 7 female) animals for a total of 56 animals. As imaging data measures between cohorts were not different at any time point, data from the two waves were combined. Weight of animals at baseline was as follows: 14 old female (FO) 222 ± 15 g; 14 old male (MO) 428 ± 20 g; 14 young female (FY) 178 ± 11 g; 14 young male (MY) 312 ± 26 g. Animals had ad libitum access to standard laboratory chow and water.

After the baseline scans, eight animals from each of the four age + sex categories were exposed to EtOH. All animals were fasted overnight, and the EtOH group underwent a modified version of the Majchrowicz EtOH-intoxication model [56] as described in previous studies [24, 25, 30, 57]. Briefly, rats received an initial "loading" dose of 5 g/kg 20% w/v EtOH via oral gavage,

then a maximum of 4 g/kg every 8 h (i.e., 2:00, 10:00, and 18:00) for 4 days. On each of the 4 days, animals were weighed, and tail vein blood samples (~300 μl) were collected at 8:00 each day to determine BALs in plasma based on direct reaction with the enzyme alcohol oxidase (Analox Instruments Ltd., UK). After the loading dose, EtOH was administered according to body weight, BALs, and behavioral evidence for intoxication [e.g., 56]. Control animals (n = 6 from each group) received consistent quantities of reverse osmosis water in volumes similar to those received by the experimental rats.

In total, five rats (three old males from wave 1 and two old females, one from each wave) did not survive binge EtOH exposure. Thus, results reported are for six controls (C) in each of the age + sex categories (i.e., FYC, FOC, MYC, MOC); eight in the young ethanol (E)-exposed groups (FYE, MYE), six in the old ethanol-exposed females (FOE); and five in the old ethanol-exposed males (MOE).

MR scanning procedures and data analysis
Schedule. All rats were scanned at baseline (scan 1), following 4 days of EtOH exposure and subsequent metabolic clearance of EtOH, ≥14 h (range: 13:30–22:30 h) after the last dose of EtOH (scan 2), and following 7 days of recovery (scan 3).

Anesthesia and monitoring. Isoflurane anesthesia was initiated at 2–3% and reduced to 1–2% at scan commencement. Rats were placed on an animal cradle equipped with built-in water circulation for body temperature control. Eye lubricant was used to anoint eyes for protection from dehydration. Silicon earplugs were affixed to protect ears from scanner gradient volume. Temperature and respiration were monitored throughout the ~2 h experiment. Animals received subcutaneous saline (10cc) for hydration at the end of the scan.

MRI acquisition. MR data were collected on a Bruker 70/16 US AVANCE III 7.0T system (Karlsruhe, Germany) with 380 mT/m gradient strength on each (X, Y, and Z) axis, slew rate of 3420 T/m/s, 16 cm bore size using a receive-only surface coil and ParaVision 6.1 software. A gradient-recalled echo (GRE) localizer scan was used to position the animals in the scanner and for graphical prescription of the subsequent scans. T2-weighted, high-resolution, TurboRare acquisition sequence: repetition time (TR) = 6774.8 ms; echo time (TE) = 33 ms; 0.2 mm isotropic voxels, matrix = 160 × 160; 2 averages; echo spacing = 11 ms; slice thickness = 0.5 mm; slice gap = 0; 64 interlaced slices; RARE factor = 16.

MRI processing. Preprocessing of each image included removal of noise [58] and inhomogeneity correction via ANTS 2.1.0 [59]. Each image was skull stripped by aligning a template to the scan via symmetric diffeomorphic registration [60] and the resulting deformation map was applied to the brain mask of the template. Image inhomogeneity correction was repeated on skull-stripped images. Bias-corrected, skull-stripped images were rigidly aligned to a template via ANTS 2.1.0 and used as input for further analysis. Structural images were segmented into CSF, gray matter, and white matter with finite mixture modeling (FMM) segmentation (ANTS *atropos*) producing a probability for each of the three tissue types for each voxel in the brain (Fig. 1). The final unit of measure for each tissue type was the integrated probability over the entire brain, yielding whole brain gray matter, white matter, and CSF volumes.

MRS acquisition. In vivo MRS scans were acquired in voxels placed in striatum or thalamus, each 3 × 3 × 3 mm with a point-resolved spin echo sequence (PRESS). The striatum was chosen because it is a node of the brain's reward circuitry, is involved in motivated behavior, and is sensitive to volume loss in

uncomplicated alcoholism [6, 7]. Further, profound sex differences have been observed in the striatum of male and female rats [61, 62]. The thalamus was similarly chosen because of demonstrated atrophy in alcoholism [63, 64] and also because our previous work using the Majchrowicz EtOH-intoxication model demonstrated decreases in tissue water transverse relaxation time and diffusivity measures selective to the thalamus [24]. For MRS, total acquisition time was 10:40 min (TR/TE = 2500/16 ms; 256 averages; 2 dummy scans; 4096 acquisition data points; spectral bandwidth 4000 Hz) with VAPOR (variable power and optimized relaxation delays) outer volume water suppression (bandwidth 200 Hz).

MRS metabolite quantification. LCModel analysis [Stephen Provencher, sp@lcmodel.CA] was run with the "water reference" option that provided reasonably meaningful absolute metabolite concentrations based on the unsuppressed water content of the voxel. The analysis window was 0.2–4.0 ppm. Data were pre-processed with zero-order phasing, referencing, and residual water line removal. Data were fitted to a linear combination of a number of metabolites in a simulated basis set designed for Bruker 7T acquisition at TE = 16 ms provided by Provencher containing alanine, creatine + phosphocreatine (tCr), glutamine (Gln), glutamate (Glu), glycerophosphorylcholine + phosphorylcholine (Cho), glutathione (GSH), inositol, lactate, N-acetylaspartate + N-acetylaspartylglutamate (NAA), scyllo-inositol, taurine, and several lipids and macromolecules. Only metabolite concentrations derived from fitted spectra consistently within average Cramér-Rao bounds <15% were considered.

Statistical analysis. Initial analysis of structural MRI data was conducted in R using a linear model (*lm*) analysis. All further analysis was conducted in JMP® Pro version 14.1.0 (SAS Institute Inc., Cary N.C., 1989–2019). For structural MRI, variables considered were whole brain, CSF, gray matter, and white matter volumes. For MRS, metabolites with average Cramer-Rao bounds below 15% were analyzed (i.e., NAA, tCr, Cho, Glu, Gln, GABA, GSH, Ins, taurine, and MM09). Baseline levels of each dependent variable were evaluated for effects of age, sex, and their interaction; for metabolites, region (i.e., striatum and thalamus) was additionally considered. Treatment effects on dependent variables were analyzed using omnibus repeated measures (time: baseline, binge, recovery) multivariate analysis of variance (MANOVA) considering age, sex, diagnosis, and their interaction with time. If the model

was significant, effects of treatment (EtOH or control) were further considered. Significance required a *p*-value = 0.017 for structural MRI (i.e., Bonferroni corrected for 3 tissue types, 0.05/3 tissue types) and a *p*-value = 0.005 for MRS metabolite (i.e., Bonferroni corrected for 10 metabolites, 0.05/10 metabolites) derived models. Follow-up MANOVAs and t-tests within each age + sex (i.e., FO, FY, MO, MY) category considered treatment only. Finally, a data-driven approach entered all variables showing treatment effects into a JMP-based cluster analysis.

RESULTS
Cumulative EtOH dose, BALs, and weights
EtOH animals were exposed to a cumulative 4-day total of EtOH as follows [mean ± standard deviation (SD)]: FOE 25.83 ± 1.94 g/kg; FYE 33.25 ± 1.46 g/kg; MOE 24.04 ± 3.32 g/kg; MYE 26.4 ± 1.49 g/kg (Supplementary Fig. 1a). Old male and old female EtOH groups were exposed to similar EtOH doses (*p* = 0.16); the young EtOH-exposed female rats tolerated a higher cumulative EtOH dose than the young EtOH-exposed male rats (*p* < 0.0001).

Across the 4 days of exposure, peak BALs in the EtOH-exposed groups were as follows (mean ± SD): FOE 424.25 ± 141.69 mg/dL; FYE 333.25 ± 109.31 mg/dL; MOE 312.54 ± 88.05 mg/dL; MYE 512.48 ± 76.09 mg/dL (Supplementary Fig. 1b). Peak BALs were nominally higher in old female than old male rats (*p* = 0.09); peak BALs were lower in young female than young male rats (*p* = 0.002).

The model for weight was significant [*F*(8,92) = 20.9, *p* < 0.0001] and showed effects of age (*p* < 0.0001), sex (*p* < 0.0001), their interaction (*p* < 0.0001), and treatment (*p* < 0.0001). At all time points, old rats weighed more than young rats, and male rats weighed more than female rats; the age-by-sex interaction indicated that the weight difference between the younger and older male rats was greater than that between the younger and older female rats. At baseline, weights were not different between EtOH and control groups. Binge EtOH exposure caused significant weight loss in the male (young *p* = 0.02, old *p* = 0.01) but not female (young *p* = 0.32, old *p* = 0.46) EtOH-exposed rats; weight persisted in being lower at the recovery time point in the old male animals (young *p* = 0.08, old *p* = 0.01).

Age and sex differences at baseline
Table 1 summarizes baseline differences in volume measures and metabolite levels as a function of age and sex. A linear model (*lm*)
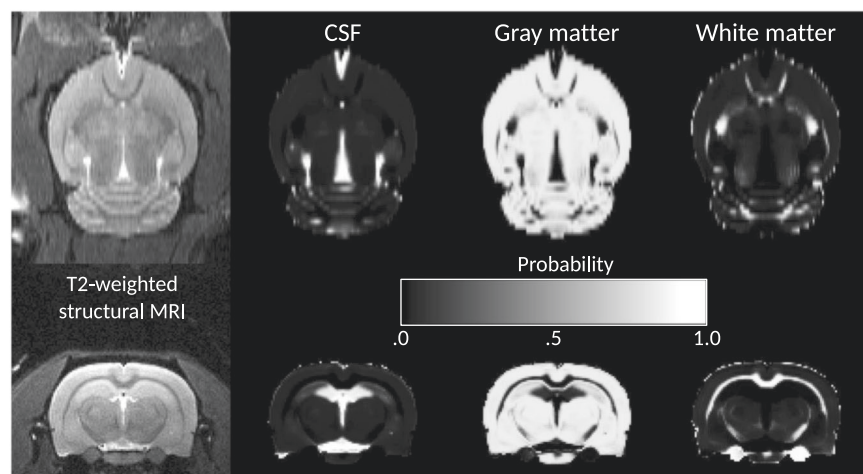
Fig. 1 Axial (top) and coronal (bottom) slices through a rat brain. From left to right are the T2-weighted structural images and the probability maps of CSF, gray matter, and white matter. The gray scale indicates the probability (0–100%) of the contents of each voxel by tissue type. The final unit of measure for each tissue type was the integrated probability over the entire brain, yielding whole brain gray matter, white matter, and CSF volumes.

Age differences in brain structural and metabolic responses to binge...
NM Zahr et al.

371

Table 1. Summary of baseline differences.

	Age	Sex	Age × sex	Region
Volumes				
Total	O > Y	M > F	Δ age M > Δ age F	n/a
CSF	O > Y	M > F	–	n/a
Gray matter	O > Y	M > F	Δ age M > Δ age F	n/a
White matter	O > Y	M > F	–	n/a
Metabolites				
NAA	O > Y	M > F	–	Thalamus > straitum
tCr	–	–	–	Thalamus > straitum
Cho	–	–	–	Thalamus > straitum
Glu	–	M > F	FY < FO; MY > MO	Thalamus > straitum
Gln	–	–	–	Thalamus > straitum
GABA	–	M > F	–	Thalamus > straitum
GSH	Y > O	F > M	–	–
Ins	O > Y	–	–	Thalamus > straitum
Taurine	–	–	–	Striatum > thalamus
MM09	–	M > F	–	Thalamus > straitum

a) Total Brain

age: t(48)=-11.7, p<.0001
sex: t(48)=16.7, p<.0001
age x sex: t(47)=-2.2, p=.03

b)

CSF
age: t(48)=-7.4, p<.0001
sex: t(48)=14.2, p<.0001
age x sex: t(47)=-0.6, p=.57

Gray Matter
age: t(48)=-8.6, p<.0001
sex: t(48)=13.4, p<.0001
age x sex: t(47)=-2.0, p=.05

White Matter
age: t(48)=-15.0, p<.0001
sex: t(48)=10.5, p<.0001
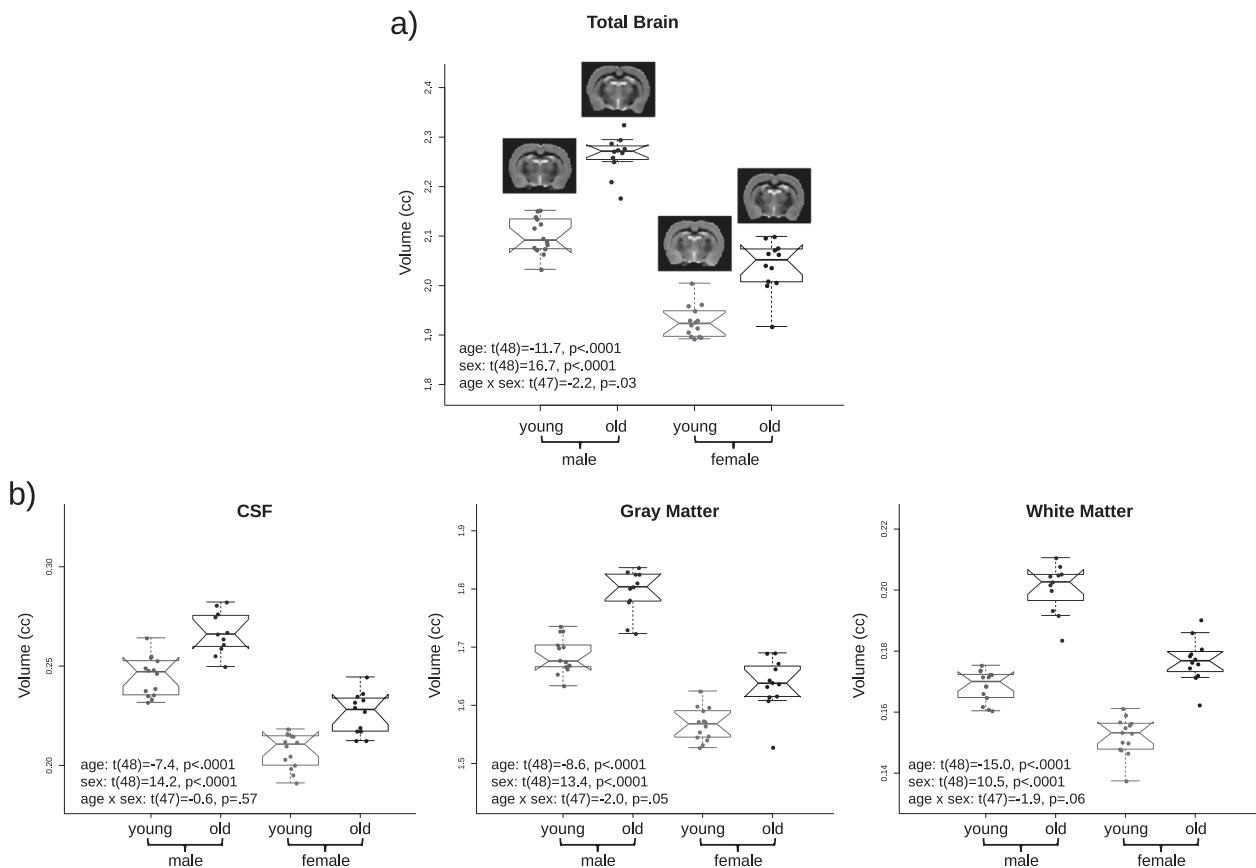age x sex: t(47)=-1.9, p=.06

Fig. 2 MRI volumes at baseline. Baseline (**a**) total brain volume and (**b**) cerebral spinal fluid (CSF), gray matter, and white matter volume for each of the age+sex categories including results of lme in R showing effects of age (greater in older than younger Fisher 344 rats), sex (greater in male than female Fisher 344 rats), and an age-by-sex interaction wherein the total volume difference between the male young and old rats was greater than that between the female young and old rats. An age-by-sex interaction was significant in gray matter and showed a trend in white matter wherein volume difference between the male young and old rats was greater than that between the female young and old rats.

analysis in R revealed that the total brain volume of the male rats was larger than that of the female rats [$t(48) = 16.7$, $p < 0.0001$] and that young rats were smaller than old rats [$t(48) = -11.7$, $p < 0.0001$] (Fig. 2). An age-by-sex interaction indicated that the volume difference between the younger and older male rats was greater than that between the female age groups [$t(47) = -2.2$, $p = 0.03$]. This age and sex pattern described each of the three constituent volumes (i.e., CSF, gray matter, white matter; Fig. 2

Age differences in brain structural and metabolic responses to binge…
NM Zahr et al.

372

Table 2. Omnibus MANOVAs.

| | Whole model | Treatment | Age | Sex | Interactions with time indicating an EtOH effect | | | |
					Treatment × time	Age × time	Sex × time	Treatment × age × sex × time
Volumes (CC)								
CSF	$F(8,92) = 7.5$, $p < 0.0001$	$F(1,46) = 7.1$, $p = 0.01$	$F(1,46) = 42.1$, $p < 0.0001$	$F(1,46) = 256.6$, $p < 0.0001$	$F(2,92) = 21.0$, $p < 0.0001$	$F(2,92) = 0.4$, $p = 0.69$	$F(2,92) = 7.1$, $p = 0.001$	$F(2,92) = 0.9$, $p = 0.42$
Gray matter	$F(8,92) = 3.7$, $p = 0.0009$	$F(1,46) = 4.5$, $p = 0.04$	$F(1,46) = 87.8$, $p < 0.0001$	$F(1,46) = 194.5$, $p < 0.0001$	$F(2,92) = 11.0$, $p < 0.0001$	$F(2,92) = 0.7$, $p = 0.49$	$F(2,92) = 1.3$, $p = 0.28$	$F(2,92) = 1.2$, $p = 0.30$
White matter	$F(8,92) = 0.5$, $p = 0.84$	$F(1,46) = 4.1$, $p = 0.05$	$F(1,46) = 285.0$, $p < 0.0001$	$F(1,46) = 149.0$, $p < 0.0001$	$F(2,92) = 1.3$, $p = 0.28$	$F(2,92) = 0.6$, $p = 0.54$	$F(2,92) = 0.0$, $p = 0.93$	$F(2,92) = 0.2$, $p = 0.79$
Metabolites (IU)								
NAA (NAA + NAAG)								
Striatum	$F(8,92) = 2.2$, $p = 0.03$	$F(1,46) = 8.7$, $p = 0.005$	$F(1,46) = 15.9$, $p = 0.0002$	$F(1,46) = 25.7$, $p < 0.0001$	$F(2,92) = 5.4$, $p = 0.006$	$F(2,92) = 0.6$, $p = 0.53$	$F(2,92) = 2.7$, $p = 0.07$	$F(2,92) = 0.1$, $p = 0.89$
Thalamus	$F(8,92) = 2.2$, $p = 0.04$	$F(1,46) = 3.2$, $p = 0.08$	$F(1,46) = 27.5$, $p < 0.0001$	$F(1,46) = 41.8$, $p < 0.0001$	$F(2,92) = 6.9$, $p = 0.002$	$F(2,92) = 0.7$, $p = 0.52$	$F(2,92) = 0.5$, $p = 0.58$	$F(2,92) = 0.1$, $p = 0.89$
tCr (Cr + PCr)								
Striatum	$F(8,92) = 4.7$, $p < 0.0001$	$F(1,46) = 7.0$, $p = 0.01$	$F(1,46) = 15.6$, $p = 0.0003$	$F(1,46) = 1.3$, $p = 0.26$	$F(2,92) = 16.2$, $p < 0.0001$	$F(2,92) = 0.2$, $p = 0.08$	$F(2,92) = 1.9$, $p = 0.15$	$F(2,92) = 0.5$, $p = 0.58$
Thalamus	$F(8,92) = 1.2$, $p = 0.32$	$F(1,46) = 1.9$, $p = 0.17$	$F(1,46) = 0.5$, $p = 0.49$	$F(1,46) = 29.0$, $p < 0.0001$	$F(2,92) = 2.1$, $p = 0.13$	$F(2,92) = 01.2$, $p = 0.30$	$F(2,92) = 0.9$, $p = 0.41$	$F(2,92) = 0.2$, $p = 0.78$
Cho (GPC + PCh)								
Striatum	$F(8,92) = 1.7$, $p = 0.11$	$F(1,46) = 0.5$, $p = 0.50$	$F(1,46) = 3.8$, $p = 0.06$	$F(1,46) = 8.1$, $p = 0.007$	$F(2,92) = 2.4$, $p = 0.10$	$F(2,92) = 1.2$, $p = 0.31$	$F(2,92) = 2.3$, $p = 0.11$	$F(2,92) = 0.8$, $p = 0.47$
Thalamus	$F(8,92) = 3.1$, $p = 0.004$	$F(1,46) = 0.0$, $p = 0.87$	$F(1,46) = 0.4$, $p = 0.53$	$F(1,46) = 10.3$, $p = 0.002$	$F(2,92) = 6.2$, $p = 0.003$	$F(2,92) = 2.2$, $p = 0.12$	$F(2,92) = 3.0$, $p = 0.05$	$F(2,92) = 0.3$, $p = 0.71$
Glu								
Striatum	$F(8,92) = 1.6$, $p = 0.14$	$F(1,46) = 1.6$, $p = 0.21$	$F(1,46) = 0.9$, $p = 0.34$	$F(1,46) = 54.5$, $p < 0.0001$	$F(2,92) = 4.0$, $p = 0.02$	$F(2,92) = 0.9$, $p = 0.41$	$F(2,92) = 0.1$, $p = 0.87$	$F(2,92) = 1.3$, $p = 0.29$
Thalamus	$F(8,92) = 0.8$, $p = 0.58$	$F(1,46) = 0.0$, $p = 0.87$	$F(1,46) = 3.0$, $p = 0.09$	$F(1,46) = 32.4$, $p < 0.0001$	$F(2,92) = 0.2$, $p = 0.81$	$F(2,92) = 0.2$, $p = 0.79$	$F(2,92) = 2.0$, $p = 0.08$	$F(2,92) = 0.3$, $p = 0.78$
Gln								
Striatum	$F(8,92) = 0.5$, $p = 0.83$	$F(1,46) = 1.0$, $p = 0.33$	$F(1,46) = 4.3$, $p = 0.05$	$F(1,46) = 0.1$, $p = 0.77$	$F(2,92) = 0.0$, $p = 0.98$	$F(2,92) = 1.0$, $p = 0.36$	$F(2,92) = 0.9$, $p = 0.39$	$F(2,92) = 0.0$, $p = 0.95$
Thalamus	$F(8,92) = 0.9$, $p = 0.53$	$F(1,46) = 2.8$, $p = 0.10$	$F(1,46) = 1.5$, $p = 0.23$	$F(1,46) = 15.8$, $p = 0.0002$	$F(2,92) = 1.6$, $p = 0.21$	$F(2,92) = 1.3$, $p = 0.27$	$F(2,92) = 0.1$, $p = .92$	$F(2,92) = 0.3$, $p = 0.74$
GABA								
Striatum	$F(8,92) = 1.5$, $p = 0.16$	$F(1,46) = 0.3$, $p = 0.56$	$F(1,46) = 2.9$, $p = 0.10$	$F(1,46) = 10.2$, $p = 0.003$	$F(2,92) = 0.0$, $p = 0.98$	$F(2,92) = 0.3$, $p = 0.76$	$F(2,92) = 5.1$, $p = 0.008$	$F(2,92) = 1.2$, $p = 0.30$
Thalamus	$F(8,92) = 2.1$, $p = 0.04$	$F(1,46) = 1.9$, $p = 0.17$	$F(1,46) = 7.8$, $p = 0.008$	$F(1,46) = 13.7$, $p = 0.0006$	$F(2,92) = 2.1$, $p = 0.13$	$F(2,92) = 2.4$, $p = 0.10$	$F(2,92) = 2.8$, $p = 0.06$	$F(2,92) = 0.4$, $p = 0.65$
GSH								
Striatum	$F(8,92) = 3.0$, $p = 0.005$	$F(1,46) = 1.1$, $p = 0.30$	$F(1,46) = 0.7$, $p = 0.41$	$F(1,46) = 29.2$, $p < 0.0001$	$F(2,92) = 10.3$, $p < 0.0001$	$F(2,92) = 0.5$, $p = 0.62$	$F(2,92) = 0.8$, $p = 0.46$	$F(2,92) = 0.6$, $p = 0.54$
Thalamus	$F(8,92) = 1.4$, $p = 0.19$	$F(1,46) = 5.5$, $p = 0.02$	$F(1,46) = 3.3$, $p = 0.08$	$F(1,46) = 1.5$, $p = 0.23$	$F(2,92) = 3.3$, $p = 0.04$	$F(2,92) = 1.4$, $p = 0.26$	$F(2,92) = 0.6$, $p = 0.56$	$F(2,92) = 0.3$, $p = 0.77$
Ins								
Striatum	$F(8,92) = 3.2$, $p = 0.003$	$F(1,46) = 22.8$, $p < 0.0001$	$F(1,46) = 147.4$, $p < 0.0001$	$F(1,46) = 3.4$, $p = 0.07$	$F(2,92) = 8.8$, $p = 0.0003$	$F(2,92) = 1.6$, $p = 0.20$	$F(2,92) = 1.3$, $p = 0.28$	$F(2,92) = 0.2$, $p = 0.81$
Thalamus	$F(8,92) = 6.8$, $p < 0.0001$	$F(1,46) = 9.8$, $p = 0.003$	$F(1,46) = 50.7$, $p < 0.0001$	$F(1,46) = 23.6$, $p < 0.0001$	$F(2,92) = 23.6$, $p < 0.0001$	$F(2,92) = 0.5$, $p = 0.59$	$F(2,92) = 0.0$, $p = 0.96$	$F(2,92) = 2.0$, $p = 0.14$
Tau								
Striatum	$F(8,92) = 3.8$, $p = 0.0006$	$F(1,46) = 32.5$, $p < 0.0001$	$F(1,46) = 24.6$, $p < 0.0001$	$F(1,46) = 6.6$, $p = 0.01$	$F(2,92) = 13.8$, $p < 0.0001$	$F(2,92) = 0.4$, $p = 0.70$	$F(2,92) = 0.3$, $p = 0.72$	$F(2,92) = 0.9$, $p = 0.39$
Thalamus	$F(8,92) = 1.0$, $p = 0.44$	$F(1,46) = 0.4$, $p = 0.53$	$F(1,46) = 5.5$, $p = 0.02$	$F(1,46) = 8.1$, $p = 0.007$	$F(2,92) = 1.1$, $p = 0.33$	$F(2,92) = 0.8$, $p = 0.47$	$F(2,92) = 0.7$, $p = 0.50$	$F(2,92) = 1.3$, $p = 0.27$
MM09								
Striatum	$F(8,92) = 0.7$, $p = 0.70$	$F(1,46) = 0.7$, $p = 0.40$	$F(1,46) = 0.5$, $p = 0.48$	$F(1,46) = 14.6$, $p = 0.0004$	$F(2,92) = 0.6$, $p = 0.56$	$F(2,92) = 1.6$, $p = 0.21$	$F(2,92) = 0.5$, $p = 0.59$	$F(2,92) = 0.1$, $p = 0.93$
Thalamus	$F(8,92) = 1.1$, $p = 0.40$	$F(1,46) = 2.2$, $p = 0.15$	$F(1,46) = 0.8$, $p = 0.39$	$F(1,46) = 0.0$, $p = 0.83$	$F(2,92) = 0.8$, $p = 0.44$	$F(2,92) = 2.3$, $p = 0.11$	$F(2,92) = 0.0$, $p = 0.98$	$F(2,92) = 0.9$, $p = 0.40$

Bold values are significant at Bonferroni-corrected p-values.

Age differences in brain structural and metabolic responses to binge…
NM Zahr et al.

373

includes statistics for these results). The age-by-sex interaction was significant only for gray matter volume, showing a trend for white matter, and was not significant for CSF.

NAA (NAA + NAAG, $F(4,107) = 144.6$, $p < 0.0001$) showed effects of age ($p < 0.0001$, old > young), sex ($p < 0.0001$, male > female), and region ($p < 0.0001$, thalamus > striatum). Glu ($F(4,107) = 19.8$, $p < 0.0001$) showed effects of sex ($p < 0.0001$, male > female), region ($p < 0.0001$, thalamus > striatum), and an age-by-sex interaction ($p = 0.02$, young female < old female; young male > old male). GABA ($F(4,107) = 29.2$, $p < 0.0001$) and MM09 ($F(4,107) = 5.2$, $p = 0.0007$) showed sex ($p < 0.007$, male > female) and region ($p < 0.002$, thalamus > striatum) effects; Ins ($F(4,107) = 84.1$, $p < 0.0001$) showed age ($p < 0.0001$, old > young) and region effects ($p < 0.0001$, thalamus > striatum). Among the 10 metabolites, only GSH ($F(4,107) = 4.0$, $p = 0.004$) showed no region effect, and age and sex effects in the opposite direction: age ($p = 0.05$, young > old) and sex ($p = 0.0008$, female > male). tCr (Cr + PCr, $F(4,107) = 47.0$, $p < 0.0001$), Cho (GPC + PCh, $F(4,107) = 17.7$, $p < 0.0001$), Gln ($F(4,107) = 6.8$, $p < 0.0001$) showed only region effects ($p < 0.0001$, thalamus > striatum); taurine ($F(4,107) = 423.1$, $p < 0.0001$) also showed only region effects, but in the opposite direction ($p < 0.0001$, striatum > thalamus).

Binge EtOH exposure and recovery effects
Omnibus MANOVAs are presented in Table 2. Significant treatment effects are summarized in Table 3. MANOVAs by each age + sex category separately are presented in Supplementary Table 1. Supplementary Table 2 compares values [mean ± SD; MRI in cubic centimeters (cc), metabolites in IU; t-tests] in EtOH-exposed and control animals. Exemplary spectra are presented in Fig. 3. Graphs of metabolites by age and sex across three time points are presented in Fig. 4 and Supplementary Fig. 2 (GABA and MM09 not presented).

The omnibus model for CSF volume was significant. All but the old females showed a treatment effect: binge EtOH exposure was associated with greater CSF volume in the EtOH-exposed relative to the control groups at the binge time point. Similarly, the omnibus model for gray matter volume was significant and showed treatment-by-time effects. All but the young females showed a treatment effect: binge EtOH exposure was associated with lower gray matter volume in the EtOH-exposed relative to the control groups at the binge time point. The model for white matter was not significant.

The overall model was not significant for **NAA** in either the striatum or thalamus. To permit comparison to previous studies, posthoc analysis showed treatment effects on striatal NAA in both male groups: binge EtOH treatment was associated with lower

NAA levels in EtOH-exposed relative to control animals at the binge time point. The model was significant for **tCr** (i.e., Cr+PCr) in striatum and showed a treatment-by-time interaction: all but old females showed treatment effects with lower tCr levels in EtOH-exposed relative to control animals at the binge time point. The model was significant for **Cho** (i.e., GPC + PCh) in thalamus and showed a treatment-by-time interaction due to young female rats: EtOH-exposed relative to their controls had lower Cho levels at the binge time point, but this was not significant with Bonferroni correction.

The full model was significant for **GSH** in striatum and showed a treatment-by-time interaction significant only in young male animals: GSH levels were lower in EtOH-exposed than control rats at the binge time point. The model for **Ins** was significant in both regions. In the striatum, all but the young females showed significant treatment effects wherein binge EtOH treatment was associated with lower levels of Ins in the EtOH-treated relative to the control animals at the binge time point. In the thalamus, all but the old male rats showed significant treatment effects with the same pattern (i.e., lower Ins in the EtOH-exposed relative to control animals at the binge time point). The model was significant for striatal **taurine** and showed effects of treatment across all 4 age + sex categories: taurine was lower in the EtOH relative to the control groups at the binge time point. The full models were not significant for Glu, Gln, GABA, or MM09 in either the striatum or thalamus.

Cluster analysis
Relations between percent change (between baseline and binge) in weight, CSF and gray matter volumes, striatal (tCr, GSH, Ins, taurine) and thalamic (Ins) metabolites showing treatment effects, and cumulative EtOH dose and peak BALs (i.e., 10 variables) were explored using cluster analysis in EtOH-exposed animals only (i.e., $n = 27$). The resulting four clusters each explained 16–17% of the overall variance: cluster 1 (16.1%) included CSF and gray matter volume; cluster 2 (17.4%) striatal and thalamic Ins and striatal tCr; cluster 3 (17.3%) peak BAL and striatal GSH and taurine; cluster 4 (16.0%) cumulative dose and weight. For cluster 1, follow-up simple regressions demonstrated an inverse relationship between CSF and gray matter volume ($r = -0.61$, $p = 0.0007$); for cluster 2, striatal Ins positively correlated with striatal tCr ($r = 0.51$, $p = 0.007$), and thalamic Ins correlated with caudate Ins ($r = 0.36$, $p = 0.06$), but no other relationships reached or approached significance. For cluster 3, striatal taurine and GSH were correlated ($r = 0.49$, $p = 0.009$), but peak BALs showed only modest inverse relationships with each of the striatal metabolites (taurine $r = -0.19$, $p = 0.15$; GSH $r = -0.29$, $p = 0.14$). Finally, cumulative dose correlated with percent change in weight ($r = 0.60$, $p = 0.0006$).

DISCUSSION
This longitudinal study of young and old, male and female Fisher 344 rats demonstrates fundamental differences based on age and sex in brain structure and neurochemical composition and further demonstrates effects of binge EtOH treatment. One caveat when comparing the current results with our earlier rodent studies of binge EtOH exposure is that previous experiments [24–26] used Wistar rats, whereas the present study used Fisher 344 rats as that is the only strain provided by the National Institute of Aging aged colony resource (https://ros.nia.nih.gov/).

Baseline differences based on age and sex
Total brain volume of male rats was larger than that of female rats and that of old rats was larger than that of young rats. This pattern was also present in the constituent tissue types (i.e., CSF, gray matter, white matter). The sex effects observed in these Fisher 344 rats are consistent with findings in humans because men as a group relative to women have larger total intracranial [65–67],

Table 3. Summary of treatment effects.

	Treatment (at binge)			
	Old female	Young female	Old male	Young male
Volume				
CSF	–	E > C	E > C	E > C
Gray matter	C > E	–	C > E	C > E
Metabolites				
Striatum				
tCr	C > E	–	C > E	C > E
GSH	–	–	–	C > E
Ins	C > E	–	C > E	C > E
Tau	C > E	C > E	C > E	C > E
Thalamus	–	–	–	–
Ins	C > E	C > E	–	C > E

Age differences in brain structural and metabolic responses to binge…
NM Zahr et al.

374

striatum

young   old   male   female

thalamus
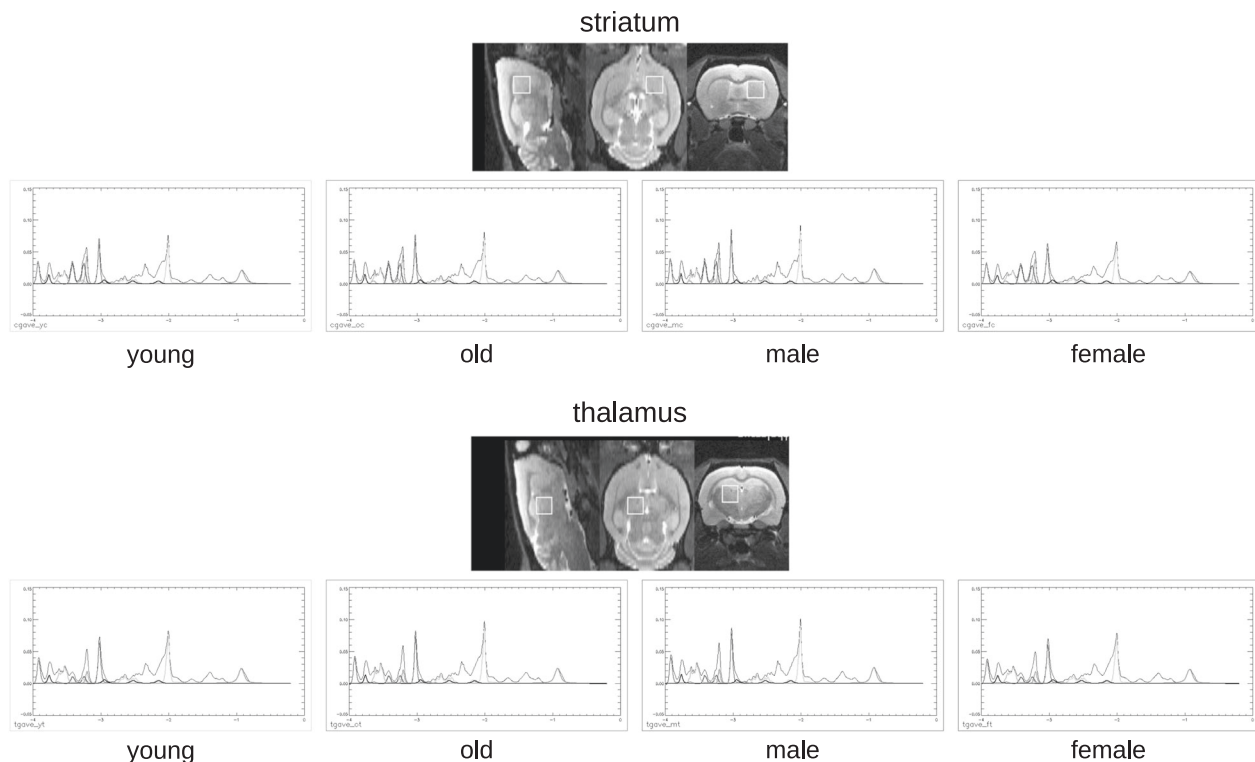

young   old   male   female

Fig. 3 Voxel locations in striatum and thalamus shown in coronal, axial, and sagittal planes. Also pictured are spectra averaged across young (light green) or old (dark green), male (blue) or female (red) categories.

cortical gray matter [68, 69], cortical white matter [70, 71], and CSF volumes [70, 72]. By contrast, larger total, gray matter, white matter, and CSF volumes in older than younger rats (i.e., continued brain growth with increasing age) diverges from human findings wherein total [e.g., 73] and gray matter volume [74–77] decreases steeply, white matter decreases but less precipitously [75, 78, 79], and CSF volume increases [72, 75] with age (generally after age 25) in both sexes [80, 81]. Evidence for continued brain growth with age in rodents comports with imaging studies conducted in alcohol-preferring male P rats tracked until 15 months of age [82] and in male Sprague-Dawley rats tracked until 13 months of age [83, also see 84–86].

With the exception of taurine, metabolite levels were higher in thalamus than striatum. Regional differences in metabolite levels are well-documented, in both human [e.g., 87, 88] and animal [e.g., 89] studies, but often, even those that include assessment of multiple regions evaluate treatment effects cross-sectionally rather than longitudinally [e.g., 90] precluding clear baseline estimates of regional differences. Previous studies in adult rats have demonstrated that taurine levels are high in striatum [relative to cortex and hippocampus, 91] and low in thalamus [relative to cerebellum and hippocampus, 92].

Metabolites that showed effects of older age included NAA, Ins, and GSH. MRS studies regarding aging effects on neurometabolite levels are equivocal [93–97] and likely related to the various methods used (ex vivo MRS studies may alter neurochemical levels during the tissue extraction and homogenization process) or to the different regions [e.g., 89, 92] or rat strains [98] evaluated. Higher NAA in the old relative to young animals comports with the observation of continued brain growth with increasing age; conversely, NAA is commonly reported to decline with aging in humans consistent with shrinking cortical volume [99]. Age-related increases in Ins [100, 101, also see 102]—a metabolite more highly concentrated in astrocytes than neurons [103]—maybe associated with age-related changes in astroglia [e.g., 104, 105]. Lower GSH was not observed in old (22-month) relative

to young (3-month) Fisher 344 rats in MRS voxels placed in cortex or hippocampus [93], but postmortem assessment found significantly lower GSH in cortex, striatum, thalamus and hippocampus of middle aged (18-month) relative to young (3-month) Fisher 344 rats [106].

For nearly all metabolites, levels were higher in male than female rats. The only exception was GSH in the striatum, for which levels were higher in the female than male rats. Higher levels of neurometabolites in male than female rats have been reported in the few studies that have included both sexes [e.g., 102, 107–109] and may be related to the relatively bigger brains (i.e., greater total volume, gray and white matter volume) of male than female rats. Higher levels of the antioxidant GSH [e.g., 110] in the female than male rats may have contributed a protective effect against the more pronounced insult to CSF and gray matter volume observed in males caused by exposure to high EtOH levels.

Effects of binge EtOH treatment

Comporting with our previous studies performed in wild-type Wistar rats [24, 25, 30, 57], binge EtOH exposure caused transient ventricular enlargement (i.e., increase in CSF volume) that was significant in the young male rats but not present in the old female rats. Thus, the current results do not support the hypothesis that following equivalent alcohol exposure protocols, older animals exhibit more brain changes than young animals and indeed, demonstrate the opposite: young animals showed a greater change in CSF volume in response to binge EtOH treatment than their older counterparts. A caveat is that five of the old, EtOH-exposed animals died during EtOH exposure, thereby precluding brain-imaging evaluation at the binge time point.

Reduced ventricular expansion and gray matter volume loss in female than male rats in response to binge EtOH treatment could not be attributed to cumulative EtOH dose administered, because the old male and female EtOH groups were exposed to similar EtOH doses and the young female relative to the young male rats
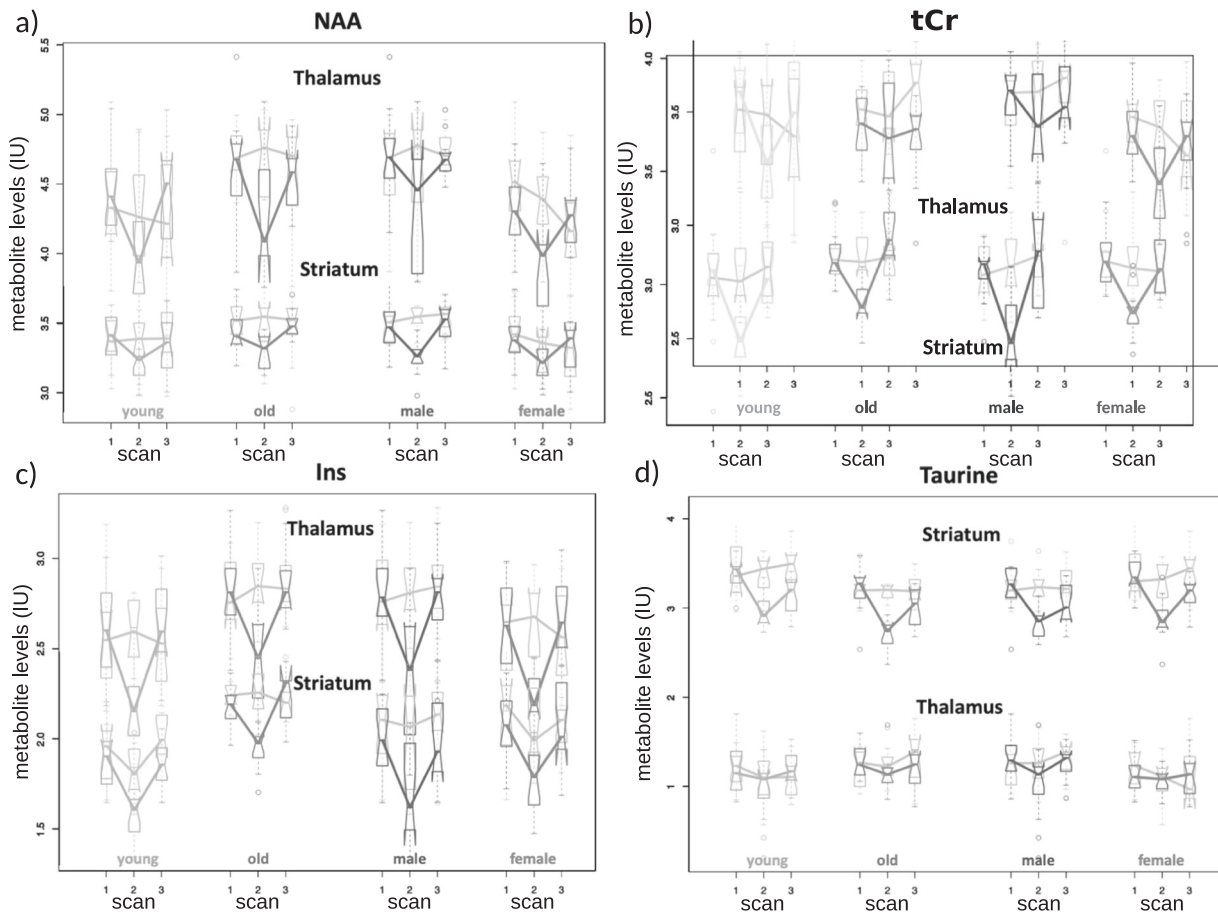
Age differences in brain structural and metabolic responses to binge…
NM Zahr et al.

375

Fig. 4 MRS-derived metabolites in thalamus and striatum. a NAA (NAA + NAAG), **b** tCr (Cr + PCr), **c** Ins, and **d** taurine levels in institutional units (IU) in the striatum and thalamus of young (light green) and old (dark green), male (blue) and female (red) groups across the three scan time points (1: baseline, 2: binge, 3: recovery; controls in gray). Note the shifted axis for tCr to permit representation of metabolite levels in both regions on a single graph. Also note taurine levels were higher in striatum than thalamus, while the opposite pattern pertained to the other three metabolites.

were exposed to a higher cumulative (relative to body weight) EtOH dose. Further, peak BALs, which were higher in the old female than male rats (though lower in the young female than male rats), cannot account for the sex differences in response to EtOH. That the young female rats had a higher cumulative dose of EtOH exposure (relative to body weight) but lower peak BALs appears to comport with the literature showing that female relative to male rats consume more EtOH [46, 47] possibly because relative to male rats, female rats have greater hepatic alcohol dehydrogenase (ADH) activity [111, 112].

Our previous studies of Wistar rats have consistently shown lower levels of NAA and tCr, and higher levels of Cho in response to binge EtOH treatment in voxels placed in dorsal hippocampus [25, 57] or whole brain [24]. The current study of Fisher 344 rats demonstrates that changes to tCr are reproducible across rat strains in the striatum. Although results of the model were not statistically significant, the NAA response in male Fisher 344 rats to high BALs was in the correct direction (lower in EtOH-treated animals relative to controls at the binge time point). Fisher 344 rats, however, did not demonstrate the predicted increase in Cho levels. The lack of an effect on Cho levels may be related to voxel location (i.e., thalamus and striatum in current study vs. hippocampus and whole brain in our previous studies) or to strain differences [e.g., 113–115] as cholinergic activity is constitutively higher in Fisher 344 relative to Wistar rats [see also 98, 116].

As this study was conducted on a higher strength magnet (7 T) than our previous spectroscopy studies (3 T) and used LCModel for

analysis, additional metabolites were evaluated. Following binge-EtOH treatment, young male rats showed reduced GSH levels in striatum [117]; Ins levels were reduced in nearly all age + sex categories in both striatum and thalamus; and taurine was reduced in all age + sex categories in the striatum. Ins is reported as reduced in rat models of liver failure [118–121], after experimental cerebral ischemia [122], oxidative stress in astrocyte extracts from the rat brain [123], and following 8- [124] or 10- [125, 126] weeks of EtOH feeding. Ins is an organic osmolyte that participates in astrocytic volume regulation [127] and release of Ins from brain cells is thought to counteract cell swelling [128]. Thus, Ins depletion in response to binge EtOH treatment could be a response of astrocytes against cell swelling following exposure to high BALs. Taurine, which similarly contributes to the regulation of neuronal and astrocytic volume [129–131], is also reduced in models of liver failure [132, 133], in experimental cerebral ischemia [134], and oxidative stress in astrocyte extracts from the rat brain [123].

Limitations
Larger sample sizes would have been desirable, but the availability of young/old matched animals was limited as were the availability and cost of MR scanning. As with all MR spectroscopy studies, there is a frequency-dependent chemical-shift displacement between water and the various metabolites such that the voxel sampled is not precisely where it is prescribed anatomically, and the displacement varies depending on how far each metabolite is from water. Nonetheless, we used fairly large voxels on large

376

structures, and the voxels as prescribed surely contained the mainstay of the target structure.

CONCLUSIONS

This study demonstrates baseline differences in brain structure and neurochemistry as a function of sex and age. Comporting with human studies, male relative to female rodent brain (total, gray, white, CSF) volumes are larger. Higher levels of NAA, Glu, and GABA in male than female rats may be associated with the larger brain size (i.e., more neurons). In contrast to the human condition, however, the rodent brain—as evidenced by total volume, gray and white matter volume, CSF volume, and NAA levels—continues to grow with older age. Ins levels higher with older age possibly reflect a compensatory mechanism, whereas GSH levels were lower with older age and may suggest loss of antioxidant activity.

Despite the use of a new strain, young male Fisher 344 rats demonstrated the pattern of ventricular enlargement and lower levels of NAA and tCr in response to binge EtOH exposure that we previously reported in young male Wistar rats. The cluster analysis showing a relation between CSF and gray matter volume changes may reveal CSF expansion at the cost of parenchymal shrinkage. The cluster analysis also supports the interpretation that neither cumulative dose nor weight directly influenced volume or metabolite levels. Instead, cumulative dose was directly related to change in weight as smaller (lower weight) animals tolerated the greatest cumulative dose. The cluster analysis showing a relationship between Ins and tCr may support a mechanism of reversible osmolarity changes due to intra- or inter- cellular fluid shifts [24] which might be due to decreased brain energy metabolism [124] in response to high BALs. Finally, higher GSH at baseline in female than male rats [135] and supports a mechanism whereby female rats may be protected against the more pronounced changes observed in male rats due to superior metabolic homeostasis mechanisms.

FUNDING AND DISCLOSURE

AUTHOR CONTRIBUTIONS
NMZ, EVS, AP contributed to the conception of the idea and designed the experiments; NMZ contributed to acquisition of data; KMP and AP contributed to analysis. NMZ drafted the manuscript; after critically reviewing it, EVS and AP revised the manuscript for important intellectual content. All authors approved the submitted version.

REFERENCES
1. Harper CG, Kril JJ, Sheedy D, Halliday GM, Double K, Dodd PR, et al. Neuropathological studies: the relationship between alcohol and aging. In: Gomberg ESL, Hegedus AM, Zucker RA, editors. Alcohol Problems and Aging. Bethesda: NIAAA; 1998. pp. 117–34.
2. Sutherland GT, Sheedy D, Kril JJ. Neuropathology of alcoholism. Handb Clin Neurol. 2014;125:603–15.
3. Buhler M, Mann K. Alcohol and the human brain: a systematic review of different neuroimaging methods. Alcohol, Clin Exp Res. 2011;35:1771–93.
4. Segobin SH, Chetelat G, Le Berre AP, Lannuzel C, Boudehent C, Vabret F, et al. Relationship between brain volumetric changes and interim drinking at six months in alcohol-dependent patients. Alcohol, Clin Exp Res. 2014;38:739–48.
5. Le Berre AP, Pitel AL, Chanraud S, Beaunieux H, Eustache F, Martinot JL, et al. Chronic alcohol consumption and its effect on nodes of frontocerebellar and limbic circuitry: comparison of effects in France and the United States. Hum Brain Mapp. 2014;35:4635–53.
6. Durazzo TC, Tosun D, Buckley S, Gazdzinski S, Mon A, Fryer SL, et al. Cortical thickness, surface area, and volume of the brain reward system in alcohol dependence: relationships to relapse and extended abstinence. Alcohol, Clin Exp Res. 2011;35:1187–200.
7. Makris N, Oscar-Berman M, Jaffin SK, Hodge SM, Kennedy DN, Caviness VS, et al. Decreased volume of the brain reward system in alcoholism. Biol Psychiatry. 2008;64:192–202.
8. Sullivan EV, Deshmukh A, De Rosa E, Rosenbloom MJ, Pfefferbaum A. Striatal and forebrain nuclei volumes: contribution to motor function and working memory deficits in alcoholism. Biol Psychiatry. 2005;57:768–76.
9. Zahr NM, Sullivan EV, Pohl KM, Pfefferbaum A, Saranathan M. Sensitivity of ventrolateral posterior thalamic nucleus to back pain in alcoholism and CD4 nadir in HIV. Human Brain Mapping. 2020;41:1351–61.
10. Grodin EN, Momenan R. Decreased subcortical volumes in alcohol dependent individuals: effect of polysubstance use disorder. Addiction Biol. 2017;22:1426–37.
11. Duka T, Gentry J, Malcolm R, Ripley TL, Borlikova G, Stephens DN, et al. Consequences of multiple withdrawals from alcohol. Alcohol, Clin Exp Res. 2004;28:233–46.
12. Pitel AL, Zahr NM, Jackson K, Sassoon SA, Rosenbloom MJ, Pfefferbaum A, et al. Signs of Preclinical Wernicke's Encephalopathy and Thiamine Levels as Predictors of Neuropsychological Deficits in Alcoholism without Korsakoff's Syndrome. Neuropsychopharmacology. 2011;36:580–8.
13. Thomson AD, Guerrini I, Bell D, Drummond C, Duka T, Field M, et al. Alcohol-related brain damage: report from a Medical Council on Alcohol Symposium, June 2010. Alcohol Alcohol. 2012;47:84–91.
14. Sullivan EV, Pfefferbaum A. Brain-behavior relations and effects of aging and common comorbidities in alcohol use disorder: a review. Neuropsychology. 2019;33:760–80.
15. Pfefferbaum A, Sullivan EV, Mathalon DH, Lim KO. Frontal lobe volume loss observed with magnetic resonance imaging in older chronic alcoholics. Alcohol, Clin Exp Res. 1997;21:521–9.
16. Fein G, Di Sclafani V, Cardenas VA, Goldmann H, Tolou-Shams M, Meyerhoff DJ. Cortical gray matter loss in treatment-naive alcohol dependent individuals. Alcohol, Clin Exp Res. 2002;26:558–64.
17. Cardenas VA, Studholme C, Meyerhoff DJ, Song E, Weiner MW. Chronic active heavy drinking and family history of problem drinking modulate regional brain tissue volumes. Psychiatry Res. 2005;138:115–30.
18. Pfefferbaum A, Zahr NM, Sassoon SA, Kwon D, Pohl KM, Sullivan EV. Accelerated and premature aging characterizing regional cortical volume loss in human immunodeficiency virus infection: contributions from alcohol, substance use, and hepatitis C coinfection. Biol Psychiatry Cogn Neurosci Neuroimaging. 2018;3:844–59.
19. Sullivan EV, Zahr NM, Sassoon SA, Thompson WK, Kwon D, Pohl KM, et al. The role of aging, drug dependence, and hepatitis C comorbidity in alcoholism cortical compromise. JAMA Psychiatry. 2018;75:474–83.
20. Zahr NM, Pohl KM, Saranathan M, Sullivan EV, Pfefferbaum A. Hippocampal subfield CA2+3 exhibits accelerated aging in alcohol use disorder: a preliminary study. Neuroimage Clin. 2019;22:101764.
21. Breslow RA, Castle IP, Chen CM, Graubard BI. Trends in Alcohol Consumption Among Older Americans: National Health Interview Surveys, 1997 to 2014. Alcohol, Clin Exp Res. 2017;41:976–86.
22. Grant BF, Chou SP, Saha TD, Pickering RP, Kerridge BT, Ruan WJ, et al. Prevalence of 12-Month Alcohol Use, High-Risk Drinking, and DSM-IV Alcohol Use Disorder in the United States, 2001-2002 to 2012-2013: Results From the National Epidemiologic Survey on Alcohol and Related Conditions. JAMA Psychiatry. 2017;74:911–23.
23. Pfefferbaum A, Zahr NM, Mayer D, Rohlfing T, Sullivan EV. Dynamic responses of selective brain white matter fiber tracts to binge alcohol and recovery in the rat. PLoS ONE. 2015;10:e0124885.
24. Zahr NM, Mayer D, Rohlfing T, Orduna J, Luong R, Sullivan EV, et al. A mechanism of rapidly reversible cerebral ventricular enlargement independent of tissue atrophy. Neuropsychopharmacology. 2013;38:1121–9.
25. Zahr NM, Mayer D, Rohlfing T, Hsu O, Vinco S, Orduna J, et al. Rat strain differences in brain structure and neurochemistry in response to binge alcohol. Psychopharmacology. 2014;231:429–45.
26. Zahr NM, Mayer D, Rohlfing T, Hasak M, Hsu O, Vinco S, et al. Brain injury and recovery following binge ethanol: evidence from in vivo magnetic resonance spectroscopy. Biol Psychiatry. 2010;67:846–54.
27. Pfefferbaum A, Zahr NM, Mayer D, Vinco S, Orduna J, Rohlfing T, et al. Ventricular expansion in wild-type Wistar rats after alcohol exposure by vapor chamber. Alcohol, Clin Exp Res. 2008;32:1459–67.
28. Zahr NM, Lenart A, Karpf JA, Casey KM, Pohl KM, Sullivan EV, et al. Multi-modal imaging reveals differential brain volumetric, biochemical, and white matter fiber responsivity to repeated intermittent ethanol vapor exposure in male and female rats. Neuropharmacology. 2020;170:108066.
29. Dlugos CA, Pentney RJ. Morphometric evidence that the total number of synapses on Purkinje neurons of old F344 rats is reduced after long-term ethanol treatment and restored to control levels after recovery. Alcohol Alcohol. 1997;32:161–72.

Age differences in brain structural and metabolic responses to binge...
NM Zahr et al.

377

30. Zhao Q, Fritz M, Pfefferbaum A, Sullivan EV, Pohl KM, Zahr NM. Jacobian maps reveal under-reported brain regions sensitive to extreme binge ethanol intoxication in the rat. Front Neuroanat. 2018;12:108.

31. Durazzo TC, Gazdzinski S, Rothlind JC, Banys P, Meyerhoff DJ. Brain metabolite concentrations and neurocognition during short-term recovery from alcohol dependence: preliminary evidence of the effects of concurrent chronic cigarette smoking. Alcohol, Clin Exp Res. 2006;30:539–51.

32. Mon A, Durazzo TC, Meyerhoff DJ. Glutamate, GABA, and other cortical metabolite concentrations during early abstinence from alcohol and their associations with neurocognitive changes. Drug Alcohol Depend. 2012 125:27–36.

33. Zahr NM, Mayer D, Rohlfing T, Sullivan EV, Pfefferbaum A. Imaging neuroinflammation? A perspective from MR spectroscopy. Brain Pathol. 2014;24:654–64.

34. Fievisohn EM, Vaughn BM, Hardy WN. Techniques for the investigation of traumatic brain injury mechanisms characterized by magnetic resonance spectroscopy. Biomed Sci Instrum. 2012;48:126–33.

35. Egerton A. The potential of (1)H-MRS in CNS drug development. Psychopharmacology. 2019.

36. Fritz M, Klawonn AM, Zahr NM. Neuroimaging in alcohol use disorder: From mouse to man. J Neurosci Res. PMID: 31006907, 2019.

37. Zhang XD, Zhang LJ, Wu SY, Lu GM. Multimodality magnetic resonance imaging in hepatic encephalopathy: an update. World J Gastroenterol. 2014;20:11262–72.

38. de Graaf RA. In Vivo NMR Spectroscopy: Principles and Techniques. 2nd edn. John Wiley & Sons Ltd: West Sussex; 2007.

39. Mann K, Batra A, Gunthner A, Schroth G. Do women develop alcoholic brain damage more readily than men? Alcohol, Clin Exp Res. 1992;16:1052–6.

40. Mann K, Ackermann K, Croissant B, Mundle G, Nakovics H, Diehl A. Neuroimaging of gender differences in alcohol dependence: are women more vulnerable? Alcohol, Clin Exp Res. 2005;29:896–901.

41. Randall CL, Roberts JS, Del Boca FK, Carroll KM, Connors GJ, Mattson ME. Telescoping of landmark events associated with drinking: a gender comparison. J Stud Alcohol. 1999;60:252–60.

42. Hommer D, Momenan R, Rawlings R, Ragan P, Williams W, Rio D, et al. Decreased corpus callosum size among alcoholic women. Arch Neurol. 1996;53:359–63.

43. Sullivan EV, Rohlfing T, Pfefferbaum A. Pontocerebellar volume deficits and ataxia in alcoholic men and women: no evidence for "telescoping". Psychopharmacology. 2010;208:279–90.

44. Pfefferbaum A, Rosenbloom M, Deshmukh A, Sullivan E. Sex differences in the effects of alcohol on brain structure. Am J Psychiatry. 2001;158:188–97.

45. Diehl A, Croissant B, Batra A, Mundle G, Nakovics H, Mann K. Alcoholism in women: is it different in onset and outcome compared to men? Eur Arch Psychiatry Clin Neurosci. 2007;257:344–51.

46. Moore CF, Lynch WJ. Alcohol preferring (P) rats as a model for examining sex differences in alcohol use disorder and its treatment. Pharm Biochem Behav. 2015;132:1–9.

47. Li TK, Lumeng L. Alcohol preference and voluntary alcohol intakes of inbred rat strains and the National Institutes of Health heterogeneous stock of rats. Alcohol, Clin Exp Res. 1984;8:485–6.

48. van Haaren F, Anderson K. Sex differences in schedule-induced alcohol consumption. Alcohol.1994;11:35–40.

49. Schramm-Sapyta NL, Francis R, MacDonald A, Keistler C, O'Neill L, Kuhn CM. Effect of sex on ethanol consumption and conditioned taste aversion in adolescent and adult rats. Psychopharmacology. 2014;231:1831–9.

50. Varlinskaya EI, Spear LP. Social consequences of ethanol: Impact of age, stress, and prior history of ethanol exposure. Physiol Behav. 2015;148:145–50.

51. Devaud LL, Chadda R. Sex differences in rats in the development of and recovery from ethanol dependence assessed by changes in seizure susceptibility. Alcohol, Clin Exp Res. 2001;25:1689–96.

52. Varlinskaya EI, Spear LP. Acute ethanol withdrawal (hangover) and social behavior in adolescent and adult male and female Sprague-Dawley rats. Alcohol, Clin Exp Res. 2004;28:40–50.

53. Overstreet DH, Knapp DJ, Breese GR. Similar anxiety-like responses in male and female rats exposed to repeated withdrawals from ethanol. Pharm Biochem Behav. 2004;78:459–64.

54. Reilly W, Koirala B, Devaud LL. Sex differences in acoustic startle responses and seizure thresholds between ethanol-withdrawn male and female rats. Alcohol Alcohol. 2009;44:561–6.

55. Andreollo NA, Santos EF, Araujo MR, Lopes LR. Rat's age versus human's age: what is the relationship? Arq Bras Cir Dig. 2012;25:49–51.

56. Majchrowicz E. Induction of physical dependence upon ethanol and the associated behavioral changes in rats. Psychopharmacologia. 1975;43:245–54.

57. Zahr NM, Mayer D, Rohlfing T, Hasak MP, Hsu O, Vinco S, et al. Brain injury and recovery following binge ethanol: evidence from in vivo magnetic resonance spectroscopy. Biol Psychiatry. 2010;67:846–54.

58. Coupe P, Yger P, Prima S, Hellier P, Kervrann C, Barillot C. An optimized blockwise nonlocal means denoising filter for 3-D magnetic resonance images. IEEE Trans Med Imaging. 2008;27:425–41.

59. Tustison NJ, Avants BB, Siqueira M, Gee JC. Topological well-composedness and glamorous glue: a digital gluing algorithm for topologically constrained front propagation. IEEE transactions on image processing: a publication of the IEEE Signal Processing. Society. 2011;20:1756–61.

60. Tustison NJ, Avants BB, Cook PA, Zheng Y, Egan A, Yushkevich PA, et al. N4ITK: improved N3 bias correction. IEEE Trans Med Imaging. 2010;29:1310–20.

61. Andersen SL, Rutstein M, Benzo JM, Hostetter JC, Teicher MH. Sex differences in dopamine receptor overproduction and elimination. Neuroreport. 1997;8:1495–8.

62. Becker JB, Ramirez VD. Experimental studies on the development of sex differences in the release of dopamine from striatal tissue fragments in vitro. Neuroendocrinology. 1981;32:168–73.

63. Harding A, Halliday G, Caine D, Kril J. Degeneration of anterior thalamic nuclei differentiates alcoholics with amnesia. Brain. 2000;123(Pt 1):141–54.

64. Pitel AL, Chetelat G, Le Berre AP, Desgranges B, Eustache F, Beaunieux H. Macrostructural abnormalities in Korsakoff syndrome compared with uncomplicated alcoholism. Neurology. 2012;78:1330–3.

65. Chen X, Sachdev PS, Wen W, Anstey KJ. Sex differences in regional gray matter in healthy individuals aged 44-48 years: a voxel-based morphometric study. NeuroImage. 2007;36:691–9.

66. Pell GS, Briellmann RS, Chan CH, Pardoe H, Abbott DF, Jackson GD. Selection of the control group for VBM analysis: influence of covariates, matching and sample size. NeuroImage. 2008;41:1324–35.

67. Luders E, Toga AW. Sex differences in brain anatomy. Prog Brain Res. 2010;186:3–12.

68. Sullivan EV, Rosenbloom M, Serventi KL, Pfefferbaum A. Effects of age and sex on volumes of the thalamus, pons, and cortex. Neurobiol Aging. 2004;25:185–92.

69. Narvacan K, Treit S, Camicioli R, Martin W, Beaulieu C. Evolution of deep gray matter volume across the human lifespan. Hum Brain Mapp. 2017;38:3771–90.

70. Gur RC, Turetsky BI, Matsui M, Yan M, Bilker W, Hughett P, et al. Sex differences in brain gray and white matter in healthy young adults: correlations with cognitive performance. J Neurosci. 1999;19:4065–72.

71. Passe TJ, Rajagopalan P, Tupler LA, Byrum CE, MacFall JR, Krishnan KR. Age and sex effects on brain morphology. Prog Neuro-Psychopharmacol Biol Psychiatry. 1997;21:1231–7.

72. Grant R, Condon B, Lawrence A, Hadley DM, Patterson J, Bone I, et al. Human cranial CSF volumes measured by MRI: sex and age influences. Magn Reson imaging. 1987;5:465–8.

73. Liu RS, Lemieux L, Bell GS, Sisodiya SM, Shorvon SD, Sander JW, et al. A longitudinal study of brain morphometrics using quantitative magnetic resonance imaging and difference image analysis. NeuroImage. 2003;20:22–33.

74. Condon B, Grant R, Hadley D, Lawrence A. Brain and intracranial cavity volumes: in vivo determination by MRI. Acta Neurol Scand. 1988;78:387–93.

75. Pfefferbaum A, Mathalon DH, Sullivan EV, Rawles JM, Zipursky RB, Lim KO. A quantitative magnetic resonance imaging study of changes in brain morphology from infancy to late adulthood. Arch Neurol. 1994;51:874–87.

76. Taki Y, Thyreau B, Kinomura S, Sato K, Goto R, Kawashima R, et al. Correlations among brain gray matter volumes, age, gender, and hemisphere in healthy individuals. PLoS ONE. 2011;6:e22734.

77. Van Laere KJ, Dierckx RA. Brain perfusion SPECT: age- and sex-related effects correlated with voxel-based morphometric findings in healthy adults. Radiology. 2001;221:810–7.

78. Guttmann CR, Jolesz FA, Kikinis R, Killiany RJ, Moss MB, Sandor T, et al. White matter changes with normal aging. Neurology. 1998;50:972–8.

79. Allen JS, Bruss J, Brown CK, Damasio H. Normal neuroanatomical variation due to age: the major lobes and a parcellation of the temporal region. Neurobiol Aging. 2005;26:1245–60.

80. Resnick SM, Pham DL, Kraut MA, Zonderman AB, Davatzikos C. Longitudinal magnetic resonance imaging studies of older adults: a shrinking brain. J Neurosci. 2003;23:3295–301.

81. Pfefferbaum A, Rohlfing T, Rosenbloom MJ, Chu W, Colrain IM, Sullivan EV. Variation in longitudinal trajectories of regional brain volumes of healthy men and women (ages 10 to 85 years) measured with atlas-based parcellation of MRI. NeuroImage. 2013;65:176–93.

82. Sullivan EV, Adalsteinsson E, Sood R, Mayer D, Bell R, McBride W. et al. Longitudinal brain magnetic resonance imaging study of the alcohol-preferring rat. Part I: adult brain growth. Alcohol, Clin Exp Res. 2006;30:1234–47.

Age differences in brain structural and metabolic responses to binge...
NM Zahr et al.

378

83. Tang H, Vasselli JR, Wu EX, Boozer CN, Gallagher D. High-resolution magnetic resonance imaging tracks changes in organ and tissue mass in obese and aging rats. Am J Physiol Regul Integr Comp Physiol. 2002;282:R890–9.

84. Vetreno RP, Yaxley R, Paniagua B, Johnson GA, Crews FT. Adult rat cortical thickness changes across age and following adolescent intermittent ethanol treatment. Addiction Biol. 2017;22:712–23.

85. Calabrese F, Guidotti G, Racagni G, Riva MA. Reduced neuroplasticity in aged rats: a role for the neurotrophin brain-derived neurotrophic factor. Neurobiol Aging. 2013;34:2768–76.

86. Hamezah HS, Durani LW, Ibrahim NF, Yanagisawa D, Kato T, Shiino A, et al. Volumetric changes in the aging rat brain and its impact on cognitive and locomotor functions. Exp Gerontol. 2017;99:69–79.

87. Zahr NM, Mayer D, Pfefferbaum A, Sullivan EV. Low striatal glutamate levels underlie cognitive decline in the elderly: evidence from in vivo molecular spectroscopy. Cereb Cortex. 2008;18:2241–50.

88. Zahr NM, Mayer D, Rohlfing T, Chanraud S, Gu M, Sullivan EV, et al. In vivo glutamate measured with magnetic resonance spectroscopy: behavioral correlates in aging. Neurobiol Aging. 2013;34:1265–76.

89. Mayer D, Zahr NM, Sullivan EV, Pfefferbaum A. In vivo metabolite differences between the basal ganglia and cerebellum of the rat brain detected with proton MRS at 3T. Psychiatry Res-Neuroimaging. 2007;154:267–73.

90. Adriani W, Canese R, Podo F, Laviola G. 1H MRS-detectable metabolic brain changes and reduced impulsive behavior in adult rats exposed to methylphenidate during adolescence. Neurotoxicology Teratol. 2007;29:116–25.

91. Tkac I, Rao R, Georgieff MK, Gruetter R. Developmental and regional changes in the neurochemical profile of the rat brain determined by in vivo 1H NMR spectroscopy. Magn Reson Med. 2003;50:24–32.

92. Hong ST, Balla DZ, Pohmann R. Determination of regional variations and reproducibility in in vivo 1H NMR spectroscopy of the rat brain at 16.4 T. Magn Reson Med. 2011;66:11–7.

93. Harris JL, Yeh HW, Swerdlow RH, Choi IY, Lee P, Brooks WM. High-field proton magnetic resonance spectroscopy reveals metabolic effects of normal brain aging. Neurobiol Aging. 2014;35:1686–94.

94. Aureli T, Miccheli A, Ricciolini R, Di Cocco ME, Ramacci MT, Angelucci L, et al. Aging brain: effect of acetyl-L-carnitine treatment on rat brain energy and phospholipid metabolism. A study by 31P and 1H NMR spectroscopy. Brain Res. 1990;526:108–12.

95. Katz-Brull R, Koudinov AR, Degani H. Choline in the aging brain. Brain Res. 2002;951:158–65.

96. Driscoll I, Howard SR, Stone JC, Monfils MH, Tomanek B, Brooks WM, et al. The aging hippocampus: a multi-level analysis in the rat. Neuroscience. 2006;139:1173–85.

97. Paban V, Fauvelle F, Alescio-Lautier B. Age-related changes in metabolic profiles of rat hippocampus and cortices. Eur J Neurosci. 2010;31:1063–73.

98. Hong ST, Balla DZ, Choi C, Pohmann R. Rat strain-dependent variations in brain metabolites detected by in vivo (1) H NMR spectroscopy at 16.4T. NMR Biomed. 2011;24:1401–7.

99. Cleeland C, Pipingas A, Scholey A, White D. Neurochemical changes in the aging brain: A systematic review. Neurosci Biobehav Rev. 2019;98:306–19.

100. Macri MA, D'Alessandro N, Di Giulio C, Di Iorio P, Di Luzio S, Giuliani P, et al. Regional changes in the metabolite profile after long-term hypoxia-ischemia in brains of young and aged rats: a quantitative proton MRS study. Neurobiol Aging. 2006;27:98–104.

101. Macri MA, D'Alessandro N, Di Giulio C, Di Iorio P, Di Luzio S, Giuliani P, et al. Region-specific effects on brain metabolites of hypoxia and hyperoxia overlaid on cerebral ischemia in young and old rats: a quantitative proton magnetic resonance spectroscopy study. J Biomed Sci. 2010;17:14.

102. Zhang X, Liu H, Wu J, Zhang X, Liu M, Wang Y. Metabonomic alterations in hippocampus, temporal and prefrontal cortex with age in rats. Neurochem Int. 2009;54:481–7.

103. Glanville NT, Byers DM, Cook HW, Spence MW, Palmer FB. Differences in the metabolism of inositol and phosphoinositides by cultured cells of neuronal and glial origin. Biochimica et Biophysica Acta. 1989;1004:169–79.

104. Amenta F, Bronzetti E, Sabbatini M, Vega JA. Astrocyte changes in aging cerebral cortex and hippocampus: a quantitative immunohistochemical study. Microsc Res Tech. 1998;43:29–33.

105. Sandhir R, Onyszchuk G, Berman NE. Exacerbated glial response in the aged mouse hippocampus following controlled cortical impact injury. Exp Neurol. 2008;213:372–80.

106. Ravindranath V, Shivakumar BR, Anandatheerthavarada HK. Low glutathione levels in brain regions of aged rats. Neurosci Lett. 1989;101:187–90.

107. Liachenko S, Ramu J. Sex differences in the effect of acute administration of nicotine on MRS-measured metabolic profile of the rat brain. Neurosci Res. 2019, https://doi.org/10.1016/j.neures.2019.07.009.

108. Nilsen LH, Melo TM, Witter MP, Sonnewald U. Early differences in dorsal hippocampal metabolite levels in males but not females in a transgenic rat model of Alzheimer's disease. Neurochem Res. 2014;39:305–12.

109. Mansouri MT, Naghizadeh B, Lopez-Larrubia P, Cauli O. Gender-dependent behavioural impairment and brain metabolites in young adult rats after short term exposure to lead acetate. Toxicol Lett. 2012;210:15–23.

110. Puglia CD, Powell SR. Inhibition of cellular antioxidants: a possible mechanism of toxic cell injury. Environ Health Perspect. 1984;57:307–11.

111. Peer CJ, Strope JD, Beedie S, Ley AM, Holly A, Calis K, et al. Alcohol and aldehyde dehydrogenases contribute to sex-related differences in clearance of zolpidem in rats. Front Pharmacol. 2016;7:260.

112. Aasmoe L, Aarbakke J. Sex-dependent induction of alcohol dehydrogenase activity in rats. Biochemical Pharmacol. 1999;57:1067–72.

113. Sudakov SK, Goldberg SR, Borisova EV, Surkova LA, Turina IV, Rusakov D, et al. Differences in morphine reinforcement property in two inbred rat strains: associations with cortical receptors, behavioral activity, analgesia and the cataleptic effects of morphine. Psychopharmacology. 1993;112:183–8.

114. Herz RC, Gaillard PJ, de Wildt DJ, Versteeg DH. Differences in striatal extracellular amino acid concentrations between Wistar and Fischer 344 rats after middle cerebral artery occlusion. Brain Res. 1996;715:163–71.

115. Potier B, Lamour Y, Dutar P. Age-related alterations in the properties of hippocampal pyramidal neurons among rat strains. Neurobiol Aging. 1993;14:17–25.

116. Michalek H, Fortuna S, Pintor A. Age-related differences in brain choline acetyltransferase, cholinesterases and muscarinic receptor sites in two strains of rats. Neurobiol Aging. 1989;10:143–8.

117. Lee DW, Nam YK, Kim TK, Kim JH, Kim SY, Min JW, et al. Dose-dependent influence of short-term intermittent ethanol intoxication on cerebral neurochemical changes in rats detected by ex vivo proton nuclear magnetic resonance spectroscopy. Neuroscience. 2014;262:107–17.

118. Moats RA, Lien YH, Filippi D, Ross BD. Decrease in cerebral inositols in rats and humans. Biochemical J. 1993;295(Pt 1):15–8.

119. Chavarria L, Oria M, Romero-Gimenez J, Alonso J, Lope-Piedrafita S, Cordoba J. Brain magnetic resonance in experimental acute-on-chronic liver failure. Liver Int. 2013;33:294–300.

120. Bosoi CR, Zwingmann C, Marin H, Parent-Robitaille C, Huynh J, Tremblay M, et al. Increased brain lactate is central to the development of brain edema in rats with chronic liver disease. J Hepatol. 2014;60:554–60.

121. Rackayova V, Braissant O, McLin VA, Berset C, Lanz B, Cudalbu C. ^{1}H and ^{31}P magnetic resonance spectroscopy in a rat model of chronic hepatic encephalopathy: in vivo longitudinal measurements of brain energy metabolism. Metab Brain Dis. 2016;31:1303–14.

122. Nonaka M, Yoshimine T, Kohmura E, Wakayama A, Yamashita T, Hayakawa T. Changes in brain organic osmolytes in experimental cerebral ischemia. J Neurological Sci. 1998;157:25–30.

123. Brand A, Leibfritz D, Richter-Landsberg C. Oxidative stress-induced metabolic alterations in rat brain astrocytes studied by multinuclear NMR spectroscopy. J Neurosci Res. 1999;58:576–85.

124. Braunova Z, Kasparova S, Mlynarik V, Mierisova S, Liptaj T, Tkac I, et al. Metabolic changes in rat brain after prolonged ethanol consumption measured by 1H and 31P MRS experiments. Cell Mol Neurobiol. 2000;20:703–15.

125. Lee DW, Kim SY, Lee T, Nam YK, Ju A, Woo DC, et al. Ex vivo detection for chronic ethanol consumption-induced neurochemical changes in rats. Brain Res. 2012;1429:134–44.

126. Lee DW, Kim SY, Kim JH, Lee T, Yoo C, Nam YK, et al. Quantitative assessment of neurochemical changes in a rat model of long-term alcohol consumption as detected by in vivo and ex vivo proton nuclear magnetic resonance spectroscopy. Neurochemistry Int. 2013;62:502–9.

127. Kirk K, Strange K. Functional properties and physiological roles of organic solute channels. Annu Rev Physiol. 1998;60:719–39.

128. Haussinger D, Laubenberger J, vom Dahl S, Ernst T, Bayer S, Langer M, et al. Proton magnetic resonance spectroscopy studies on human brain myo-inositol in hypoosmolarity and hepatic encephalopathy. Gastroenterology. 1994;107:1475–80.

129. Oja SS, Saransaari P. Significance of taurine in the brain. Adv Exp Med Biol. 2017;975(Pt 1):89–94.

130. Lien YH, Shapiro JI, Chan L. Study of brain electrolytes and organic osmolytes during correction of chronic hyponatremia. Implications for the pathogenesis of central pontine myelinolysis. J Clin Investig. 1991;88:303–9.

131. Zwingmann C, Leibfritz D. Ammonia toxicity under hyponatremic conditions in astrocytes: de novo synthesis of amino acids for the osmoregulatory response. Neurochemistry Int. 2005;47:39–50.

132. Zwingmann C, Chatauret N, Rose C, Leibfritz D, Butterworth RF. Selective alterations of brain osmolytes in acute liver failure: protective effect of mild hypothermia. Brain Res. 2004;999:118–23.

Age differences in brain structural and metabolic responses to binge...
NM Zahr et al.

379

133. Peeling J, Shoemaker L, Gauthier T, Benarroch A, Sutherland GR, Minuk GY. Cerebral metabolic and histological effects of thioacetamide-induced liver failure. Am J Physiol. 1993;265(3 Pt 1):G572–8.

134. Brulatout S, Meric P, Loubinoux I, Borredon J, Correze JL, Roucher P, et al. A one-dimensional (proton and phosphorus) and two-dimensional (proton) in vivo NMR spectroscopic study of reversible global cerebral ischemia. J Neurochem. 1996;66:2491–9.

135. Chen Y, Golla S, Garcia-Milian R, Thompson DC, Gonzalez FJ, Vasiliou V. Hepatic metabolic adaptation in a murine model of glutathione deficiency. Chem Biol Interact. 2019;303:1–6.